RECORD

Volume 1

26th Annual
IEEE Power Electronics
Specialists Conference

Formerly
POWER CONDITIONING SPECIALISTS CONFERENCE 1970-71
POWER PROCESSING AND ELECTRONIC SPECIALISTS CONFERENCE 1972

The 1995 PESC is Sponsored by the

IEEE POWER ELECTRONICS SOCIETY

95CH35818

PRINTED IN THE UNITED STATES OF AMERICA

The *Power Electronics Specialists Conference Records* are publications of the IEEE Aerospace and Power Electronics Societies and are published in conformance with and pursuant to the policies of the Societies. "Power Electronics Specialist Conference" has now been adopted as a technically descriptive and professionally dignified title for the conference. Titles of previous conference records reflected attempts to find a good title for the conference. Records of the previous conferences may be obtained from: IEEE Service Center, 445 Hoes Lane, P.O. Box 1331, Piscataway, NJ 08855-1331.

Year	Catalog Number	Title
1970	70C31-AES	Power Conditioning Specialists Conference -- 1970 Record
1971	71C15-AES	Power Conditioning Specialists Conference -- 1971 Record
1972	72CHO-652-8 AES	IEEE Power Processing and Electronics Specialists Conference -- 1972 Record
1973	73CHO-787-2 AES	IEEE Power Electronics Specialists Conference -- 1973 Record
1974	74CHO-863-1 AES	IEEE Power Electronics Specialists Conference -- 1974 Record
1975	75CHO-965-4 AES	IEEE Power Electronics Specialists Conference -- 1975 Record
1976	76CH-1084-3 AES	IEEE Power Electronics Specialists Conference -- 1976 Record
1977	77CH-1213-8 AES	IEEE Power Electronics Specialists Conference -- 1977 Record
1978	78CH-1337-5 AES	IEEE Power Electronics Specialists Conference -- 1978 Record
1979	79CH-1461-3 AES	IEEE Power Electronics Specialists Conference -- 1979 Record
1980	80CH-1529-7 AES	IEEE Power Electronics Specialists Conference -- 1980 Record
1981	81CH-1652-7 AES	IEEE Power Electronics Specialists Conference -- 1981 Record
1982	82CH-1762-4 AES	IEEE Power Electronics Specialists Conference -- 1982 Record
1983	83CH-1877-0	IEEE Power Electronics Specialists Conference -- 1983 Record
1984	84CH-2000-8	IEEE Power Electronics Specialists Conference ---1984 Record
1985	85CH-2117-0	IEEE Power Electronics Specialists Conference -- 1985 Record
1986	86CH-2310-1	IEEE Power Electronics Specialists Conference -- 1986 Record
1987	87CH-2459-6	IEEE Power Electronics Specialists Conference -- 1987 Record
1988	88CH-2523-9	IEEE Power Electronics Specialists Conference --1988 Record
1989	89CH-2721-9	IEEE Power Electronics Specialists Conference -- 1989 Record
1990	90CH-2873-8	IEEE Power Electronics Specialists Conference -- 1990 Record
1991	91CH-3008-0	IEEE Power Electronics Specialists Conference -- 1991 Record
1992	92CH-3163-3	IEEE Power Electronics Specialists Conference -- 1992 Record
1993	93CH-3293-8	IEEE Power Electronics Specialists Conference -- 1993 Record
1994	94CH-3418-1	IEEE Power Electronics Specialists Conference -- 1994 Record

IEEE Catalog Number:	95CH-3581-8	
ISBN:	0-7803-2730-6	Softbound Edition
	0-7803-2731-4	Casebound Edition
	0-7803-2732-2	Microfiche Edition
ISSN:	0275-9306	
Library of Congress:	80-646675	

Interpolative Sigma Delta Modulators for High Frequency Power Electronic Applications

Glen Luckjiff Ian Dobson Deepak Divan
Electrical and Computer Engineering Department
University of Wisconsin-Madison
1415 Engineering Drive
Madison, WI 53706-1691
email: luckjiff@cae.wisc.edu

Abstract – Design techniques for interpolative ΣΔ modulators from communications are applied and adapted to improve the spectral characteristics of high frequency power electronic applications. Interpolative ΣΔ modulators with hexagonal quantization are proposed for 3 phase resonant dc link converters. Experimental and simulation results for a resonant dc link show significant improvements in spectral performance.

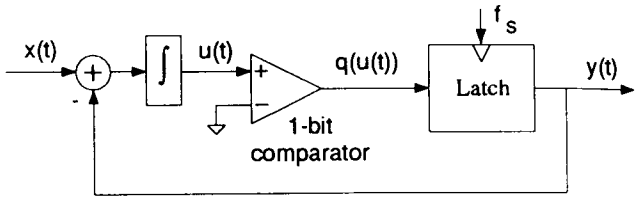

Fig. 1: Conventional sigma-delta modulator.

I. INTRODUCTION

In power electronics, simple interpolative ΣΔ modulators have been applied successfully to systems such as resonant link converters where the discrete timing of the circuit switching precludes the use of conventional modulation techniques. Resonant link converters use zero voltage switching to limit switching losses and allow much higher switching frequencies [7].

In communications, interpolative ΣΔ modulators are practical for high rate analog-to-digital conversion and data compression because of their simplicity and robustness against circuit imperfections [4]. They operate by coarsely quantizing the input signal at a sampling rate much higher than the Nyquist rate. Using a combination of feedback and integration, the resulting modulation noise is pushed to higher frequency, where it may be removed by filtering.

Converters such as the resonant link can also be thought of as analog-to-digital converters in which an analog reference is reproduced or modulated by discrete switching states. Moreover, the increased switching frequency capability of these types of converters corresponds to a high degree of oversampling. Therefore interpolative modulation techniques are pertinent to improving system performance. Over the past decade, numerous advances in interpolative ΣΔ modulation technology have appeared in the communications literature. This paper adapts and applies these improvements to the analysis and design of interpolative modulators for high frequency power electronic systems. Our experimental and simulation results demonstrate substantial improvement in spectral performance over previous work.

II. ΣΔ MODULATORS

This section explains a conventional scalar ΣΔ modulator, and how a half-bridge converter may be included in the modulator structure. These ideas are then generalized to the vector modulator of central interest in this paper.

A. *Scalar ΣΔ Modulator*

We give an example to clarify the operation of oversampled interpolative modulators. The simplest form of an interpolative modulator is the ΣΔ modulator shown in Fig. 1. x is the input signal, u is the integrator state and y is the latch output. The comparator is thought of as a quantizer whose output $q(u)$ is $\pm b$ according to the the sign of the integrator state u. The latch samples the comparator or quantizer output $q(u)$ at rate f_s and holds that signal until the next sampling instant.

Intuitively, the ΣΔ modulator uses feedback to lock onto a scalar band-limited input signal $x(t)$. As explained in [5], "Unless the input signal $x(t)$ exactly equals one of the discrete quantizer output levels, a tracking error results. The integrator accumulates the tracking error over time and the quantizer and latch feed back a value that will minimize the accumulated tracking error. Thus the quantizer output $y(t)$ toggles about the input signal $x(t)$ so that the average quantizer output is approximately equal to the average of the input."

An equivalent discrete time model of a scalar ΣΔ modulator is given by the following nonlinear difference equation:

$$u_{n+1} = x_n - q(u_n) + u_n \qquad (1)$$

where x is the input signal, u is the integrator state, and

0-7803-2730-6/95 $4.00 © 1995 IEEE

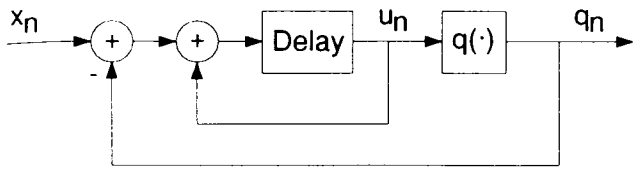

Fig. 2: Discrete-time equivalent of the ΣΔ modulator.

q is the output of the quantizer (Fig. 2):

$$q(u) = \begin{cases} +b & u \geq 0 \\ -b & u < 0 \end{cases} \tag{2}$$

The quantizer q can be understood as mapping its input u to $+b$ or $-b$ depending on which is nearest to the input. Thus q is a nearest neighbor quantizer.

To illustrate how a power electronic circuit can be embedded in a ΣΔ modulator, consider the modulator for the half-bridge converter shown in Fig. 3. In this arrangement the comparator, gating circuitry, and half-bridge of Fig. 3 replace the comparator in Fig. 1 (the placing of the latch is also changed). The comparator and latch set the switch state for each sampling period $\tau = 1/f_s$ according to the sign of the input u at the sampling instant. Now the switch state impresses $\{\pm b\}$ on the output voltage $y(t)$. Since Fig. 3 and Fig. 1 are different implementations of the same overall quantizing and latch functions, the corresponding modulators have identical behavior. Thus, by taking the input signal $x(t)$ to be the desired output voltage, the actual output voltage $y(t)$ will approximate the desired output voltage. As will be seen, this approximation can be improved by generalizing the integrator in Fig. 1 to a linear filter or by increasing the switching frequency.

The modulator described in this section is a special case of the block diagram shown in Fig. 4 (the comparator of Fig. 1 is regarded as a quantizer in Fig. 4).

B. *Vector ΣΔ Modulators with Hexagonal Quantization*

We now consider ΣΔ modulators which include conventional 3 phase voltage source inverters. In this case, all the signals in Fig. 4 become vectors. We assume a balanced representation of the signals by vectors with two coordinates (d-q) or, equivalently, by vectors with three coordinates (a-b-c) which sum to zero. The outputs of

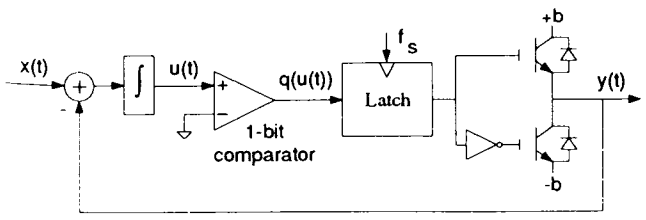

Fig. 3: ΣΔ modulator for a half-bridge converter.

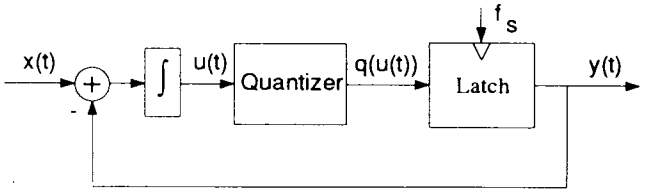

Fig. 4: General sigma-delta modulator.

the voltage source inverter are the line-to-neutral voltages which may equal one of seven possible values according to the switch state. These seven space vectors are shown as dots in Fig. 5 and can be thought of as the possible output vectors of a quantizer. Here we choose the quantizer so that a quantizer input vector u maps to the dot nearest to u. The broken lines in Fig. 5 delimit the regions which map to each dot. This "hexagonal" vector quantizer is a nearest neighbor quantizer and is well known in communications [6]. Moreover, this quantizer is optimal in the sense that the mean-square error from input to output is minimized [6].

A ΣΔ modulator for voltage source inverters is obtained by replacing the quantizer block in Fig. 4 with the hexagonal quantizer of Fig. 5, gating circuitry, and the voltage source inverter (the latch is placed between the hexagonal quantizer and the gating circuitry). This vector ΣΔ modulator with nearest neighbor hexagonal quantization is a straightforward generalization of the scalar ΣΔ modulator discussed in the previous section.

We note that a similar modulator was suggested by Habetler in [9] for application to resonant link converters and the hexagonal quantizer was also derived based on its one step ahead optimality properties by Seidl [13]. In the remainder of the paper, we show that generalizations of the ΣΔ modulator with hexagonal quantization can yield significant improvements in the spectral performance of 3 phase converters.

III. Interpolative ΣΔ Modulators

A. *White Noise Approximation*

For some design purposes, the operation of the ΣΔ modulator (Fig. 1) is analyzed by modeling the integrator with its discrete-time equivalent and the quantizer by an additive noise source $e(z)$ as shown in Fig. 6. The quantization noise $e(z)$ is the z-transform of the quantization error sequence e_n defined by $e_n = q(u_n) - u_n$.

A common approximation for scalar modulators is that the quantization noise $e(z)$ is a white, uniform noise source which is statistically uncorrelated with the input. This assumption can often be justified if the input signal or the modulator is sufficiently complex to decorrelate the noise source from the input signal. However, for dc inputs to simple modulators such as the scalar modulator of section II.A., the quantization noise spectrum consists of discrete spikes whose amplitudes and frequencies are

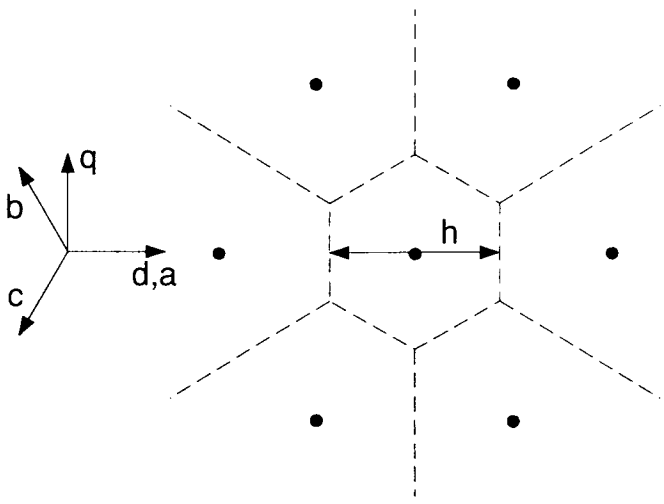

Fig. 5: The seven dots are the quantizer outputs and switching states. Each input vector is mapped to the nearest dot.

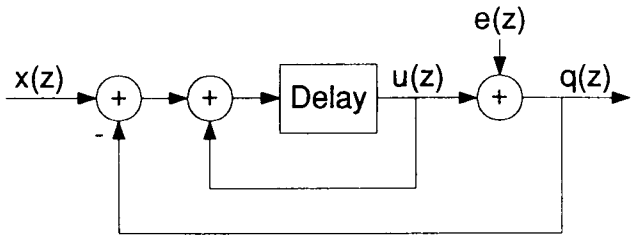

Fig. 6: Discrete-time model of the $\Sigma\Delta$ modulator. The quantizer is modeled by an additive noise source.

correlated with the input signal [8]. Nevertheless, practical design of modulators for A/D conversion often uses the quantization noise approximation [2, 1, 5].

We expect that similar considerations apply to the vector modulators described in this paper, and we assume for the purpose of design that the vector quantization noise e is a white, uniform noise source which is statistically uncorrelated with the input. This assumption greatly simplifies analysis since the resulting system is linear and conventional linear system techniques may be applied to deduce aspects of the modulator behavior and performance.

B. *Noise-Shaping*

To introduce noise shaping we review the scalar $\Sigma\Delta$ modulator example (Fig. 1). The discrete time linear model of the scalar $\Sigma\Delta$ modulator with quantization noise sequence $e(z)$ and input sequence $x(z)$ is

$$q(z) = z^{-1}x(z) + (1 - z^{-1})e(z). \qquad (3)$$

That is, the quantizer output sequence $q(z)$ is the sum of the input signal $x(z)$, delayed, plus a difference (a discrete time derivative) of the quantization noise $e(z)$.

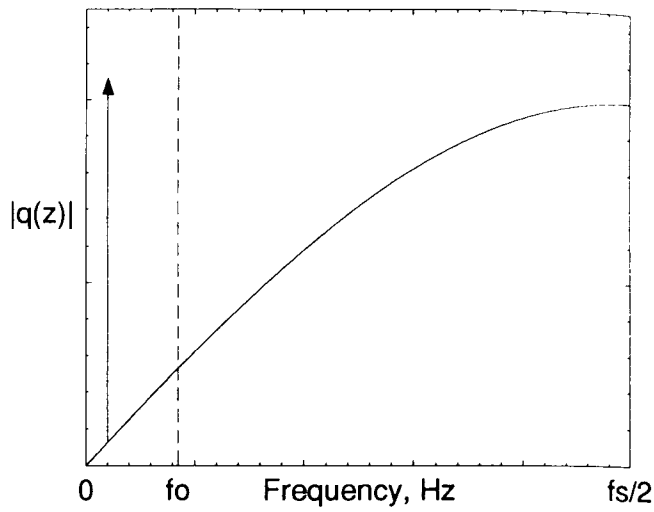

Fig. 7: Output spectrum $|q(z)|$ for $\Sigma\Delta$ modulator.

We call the frequency band $0 \leq f < f_o$ the baseband; it includes the frequency of the input signal and the band over which we wish to reduce noise in the output. The baseband can be chosen according to the load characteristics. If the input signal x is a tone (i.e. sinusoid) in the baseband, the modulator's output spectrum $|q(z)|$ is similar to that shown in Fig. 7. When the modulator is sampling much faster than the Nyquist rate $2f_o$ (i.e. oversampling), the quantization noise in the baseband will be greatly attenuated and the bulk of the noise power will be concentrated above the baseband. That is, the quantization noise will be pushed or shaped to higher frequencies. This shaping of the noise is advantageous since the high frequency noise can be removed by a low pass filter. In power electronic applications, the low pass filter may take several forms such as leakage inductance in machines and transformers or filters in uninterruptable power supplies (UPS).

To better shape the quantization noise and thus improve the spectrum in the baseband, we can replace the integrator of the $\Sigma\Delta$ modulator with more complex filters. The resulting topology is in known as an interpolative $\Sigma\Delta$ modulator and is shown in Fig. 8. Here, a linear discrete time filter $H(z)$ is placed in the modulator loop and (3) generalizes to

$$q(z) = \frac{H(z)}{1 + H(z)}x(z) + \frac{1}{1 + H(z)}e(z) \qquad (4)$$

(For example, the choice $H(z) = \frac{z^{-1}}{1-z^{-1}}$ yields the modulator of Fig. 2.) Equation (4) is a fundamental relation describing interpolative $\Sigma\Delta$ modulators. It states that the output of the modulator consists of the sum of two terms: the input signal x modified by the signal transfer function $\frac{H(z)}{1+H(z)}$ and the quantizer noise e modified by the noise transfer function $\frac{1}{1+H(z)}$. H can be designed so that the noise transfer function $\frac{1}{1+H(z)}$ is small in the baseband

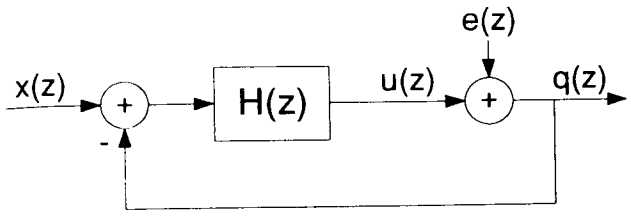

Fig. 8: Discrete time model of the interpolative $\Sigma\Delta$ modulator.

and the signal transfer function $\frac{H(z)}{1+H(z)}$ is approximately unity in the baseband. In this manner the signal-to-noise ratio in the baseband can be made large [12].

The modulator performance, which can be measured by the signal-to-noise ratio (SNR) over the baseband, is mainly governed by the "order" of the modulator and the oversampling ratio (OSR), which is the ratio of the sampling frequency to the Nyquist rate $2f_o$. Order refers to the order of the filter H. For instance, the $\Sigma\Delta$ modulator of Fig. 1 is first-order. Similarly to conventional filter design, a higher SNR requires a higher order filter and thus increased hardware complexity. The advantage of choosing a higher order filter is an improved SNR for a given OSR.

The main limitation of interpolative modulators, especially those of higher order (> 2), is their stability problems [10] in which large-amplitude low-frequency oscillations can appear. These oscillations can drive the modulator into sustained modes of integrator saturation.

C. *Noise Shaping for Vector $\Sigma\Delta$ Modulators*

Within the context developed above, modulator design consists of choosing a filter H that will ensure stability and satisfy spectral performance criteria such as a given OSR and input bandwidth. These design considerations readily generalize to vector modulators. For the vector modulator, the filter $H(z)$ has a vector input and output. Two possible choices of the filter H for use with the hexagonal quantizer of Fig. 5 are:

$$H_1 = \frac{z^{-1}}{1-z^{-1}} I \quad (5)$$

$$H_2 = \frac{z^{-1}(z^{-1}-2)}{1-2z^{-1}+z^{-2}} I \quad (6)$$

where I is an identity matrix of appropriate dimensions.

H_1 yields the first order $\Sigma\Delta$ modulator introduced in section II.A., while H_2 yields an interpolative second-order $\Sigma\Delta$ modulator. This second-order $\Sigma\Delta$ modulator is an adaptation of the modulator proposed by Candy in [3] and is superior to the first order $\Sigma\Delta$ modulator because it only requires a moderate increase in circuit complexity, and yet it achieves a 15 dB/octave tradeoff between SNR and OSR, whereas the first order $\Sigma\Delta$ modulator achieves only 9 dB/octave. Furthermore, both modulators have the same stable input range (dynamic range).

The noise-shaping filter $H(z)$ is usually designed in discrete-time. However, modulators for power electronic applications have been implemented in continuous-time with op-amps, comparators, and latches. A discrete-time modulator can be converted to an equivalent continuous-time modulator using the impulse-invariant transformation of [14].

IV. SIMULATION AND EXPERIMENTAL RESULTS

Results for the first and second order modulators proposed in section III.C. are presented. A regularly sampled 75 kHz hard-switched voltage source inverter (VSI) is simulated and experimental results for a 40 kVA, 75 kHz actively clamped resonant DC link inverter (ACRDCL) with a R-L load are presented. Although a 75 kHz VSI is not practical, its simulation provides a reference point for comparison with the experimental ACRDCL. The results are obtained with first and second order $\Sigma\Delta$ modulators specified by the nearest neighbor hexagonal quantizer and filters H_1 or H_2. A 3 phase balanced sinusoidal input with peak amplitude 0.72 (maximum is 1.0) and frequency 75 Hz is used throughout. We assume a baseband of 5 kHz which corresponds to an OSR of 7.5.

The spectra of the line-line voltage for the first and second order modulators are shown in Fig. 9 for the simulated VSI. Comparison between the two modulators shows approximately 23 dB of modulation noise improvement up to 1 kHz of the second order over the first order modulator, and the spectra converge at approximately the baseband limit frequency ($f_o = 5kHz$). For simulations, FFTs were performed on over 32,000 data points using a Blackman window. The envelopes of the voltage waveforms for the simulated VSI and the experimental ACRDCL are similar.

Fig. 10 shows the ACRDCL line-to-line voltage and line current waveforms for the first order modulator. Fig. 11 shows results of the same signals for the second order modulator. The spectra of the line-line voltage for both modulators are shown in Fig. 12 for the ACRDCL. Comparison between the two modulators shows that up to approximately 500 Hz the modulation noise for the first order modulator is approximately 5 dB less than that of the second order modulator. Beyond 500 Hz, the second order modulator shows approximately 7-10 dB of modulation noise improvement, with a maximum improvement of 12 dB at 2 kHz.

The differences between the modulation noise spectra of the VSI and the ACRDCL are perhaps due to the sampling frequency jitter (pulse width irregularity) and hardware inaccuracies which are inherent in the ACRDCL [7]. Further, the output voltage pulse of the VSI has a rectangular shape, whereas the experimental ACRDCL output voltage pulse has a clipped sinusoidal shape.

The stable input signal range for the first and second order $\Sigma\Delta$ modulators is the hexagon which passes through the outer six output space vectors of Fig. 5. When the input signal exceeds this range, the modulator's integra-

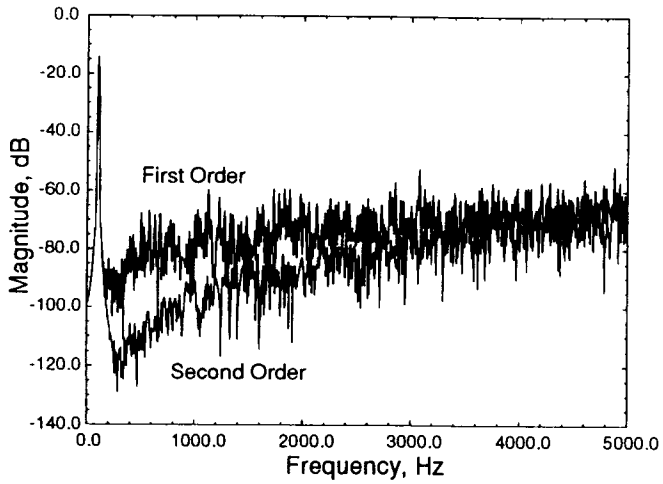

Fig. 9: Simulated VSI line-neutral voltage spectra for first and second order modulators.

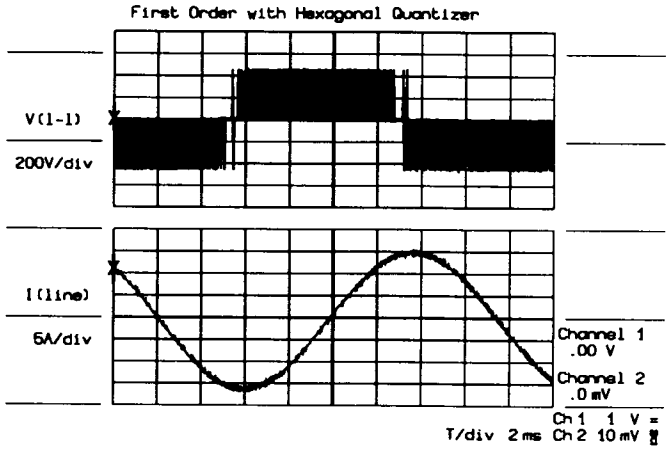

Fig. 10: Experimental ACRDCL Line-line voltage and line current for the first order modulator.

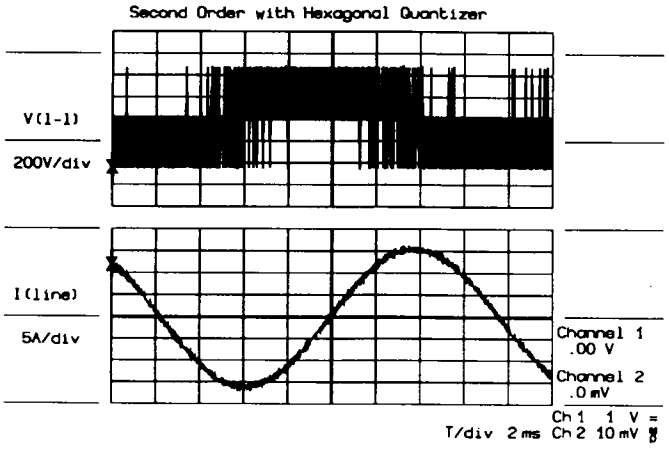

Fig. 11: Experimental ACRDCL Line-line voltage and line current for the second order modulator.

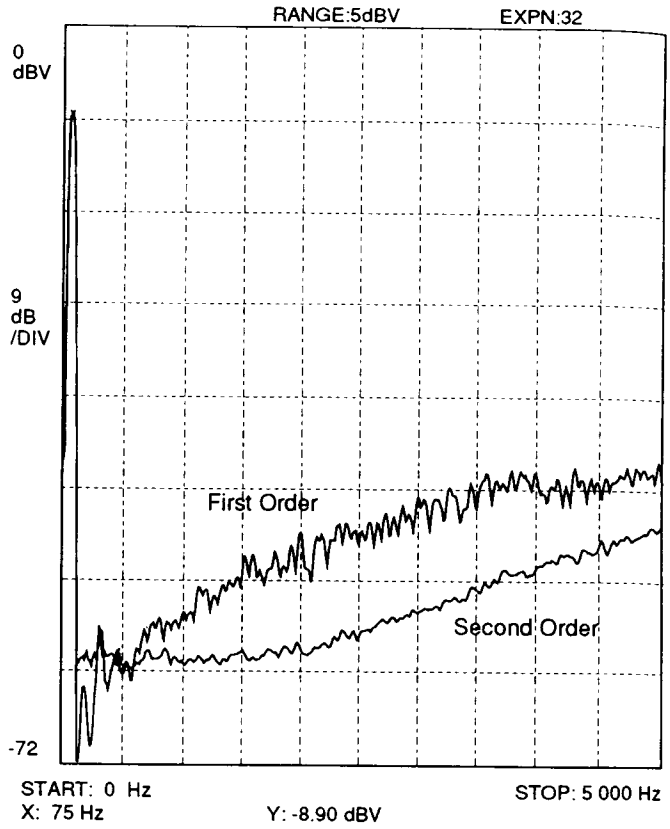

Fig. 12: Experimental ACRDCL line-line voltage spectra for first and second order modulators.

tors wind up. However, overmodulation causes the input signal to exceed the stable range. To address this problem, clippers may be placed on the integration capacitors. The thresholds of the clippers are selected to be slightly greater than the integrator voltages during stable operation. This stabilization technique ensures that the output voltage waveforms gradually degrade into six-step mode as the input signal is increased beyond the the stable input signal range. This technique may also be applied to higher-order (> 2) interpolative modulators which always have the potential for oscillation when the input exceeds the stable input range [12, 1].

V. OVERVIEW

This section explains some general features of the view of power electronics which inform our proposed modulator designs. The main analogy we exploit is with the methods in communications theory of converting an analog signal to a digital signal with a quantizer and subsequently (after transmission) converting the digital signal back to an analog signal. We think of the power electronic circuit acting as an A/D converter in which the analog input is the signal to be synthesized and the quantized digital output is the state of the circuit switches. In a voltage

source circuit, the switches impress discrete voltages on the load. Then the low-pass filtering action of typical loads remove the modulation frequencies and hence convert these discrete voltages back to analog form. In both communications theory and power electronics, the aim is to design the system so that the input signal is passed through the system with minimal distortion from noise.

One consequence of this interpretation is that the power electronic switching states determine the possible "digitized states" or quantizer outputs. For example, the voltage source inverter has seven switching states which correspond to the seven output vectors in Fig. 5. Similarly, other circuits such as the matrix converter, multilevel converters, and multiphase converters define particular quantizer outputs.

Although the quantizer outputs are determined by the power electronic circuit, the modulator designer may choose the set of input vectors which map to each quantizer output. The quantizers presented so far are nearest neighbor quantizers which map each input to the nearest output. However, other choices are possible. For example, consider the hexagonal quantizer of Fig. 5. Here, the parameter h determines the size of the inner hexagonal region and may be altered to obtain another quantizer.

Setting h to zero eliminates the central output vector entirely and the resulting circuit is simplified because the number of comparators required is reduced from nine to three. However, the penalty for this circuit simplification is significant for the first order modulator and relatively small for the second order modulator. A similar discussion for scalar first and second order modulators is in [11].

Viewing high frequency power electronic circuits as contributing to quantization allows them to be regarded as part of the interpolative modulator topology (Fig. 8). It follows that noise-shaping methods of filter design may be applied to optimize the spectral characteristics.

The first and second order vector $\Sigma\Delta$ modulators proposed in section III.C. demonstrate the feasibility of designing converters using methods from communications. Higher order interpolative $\Sigma\Delta$ modulator architectures [1, 5] and stability issues [10, 12] are discussed extensively in the communications literature. We have found that these more complex architectures can similarly be extended to the vector case and in particular to modulators with hexagonal quantization.

VI. CONCLUSION

This paper formulates the problem of reproducing a desired signal with a high frequency power electronic circuit by regarding the circuit as performing quantization in an interpolative $\Sigma\Delta$ modulator. The binary quantizers of conventional scalar $\Sigma\Delta$ modulators generalize easily to the vector quantizers appropriate to power electronic circuit topologies. For example, a nearest neighbor hexagonal quantizer is one obvious choice for a 3 phase voltage source inverter. Linear design methods from communications theory can then be applied to shape the quantization noise so that it is pushed to higher frequencies and will be attenuated by the load. First and second order modulator designs are proposed for a voltage source inverter and are tested experimentally on a resonant dc link. These examples show that the approach yields significant improvements in spectral performance.

ACKNOWLEDGMENT

We thank Mukul Chandorkar, Alexander Julian, Gautam Sinha, and Ian Wallace for their assistance and helpful comments. Funding in part from NSF PYI grant ECS-9157192 is gratefully acknowledged.

References

[1] R.W. Adams. Design and implementation of an audio 18 bit analog to digital converter using oversampling techniques. *J. Audio Eng. Soc.*, 34(3):153–166, March 1986.

[2] R.W. Adams, P.F. Ferguson, A. Ganesan, S. Vincelette, A. Volpe, and R. Libert. Theory and practical implementation of a fifth order sigma delta A/D converter. *J. Audio Eng. Soc.*, 39(7):515–528, July 1991.

[3] J.C. Candy. A use of double integration in sigma delta modulation. *IEEE Trans. Commun.*, COM-33(3):249–258, March 1985.

[4] J.C. Candy and G.C. Temes. *Oversampling Methods for A/D and D/A Conversion*, chapter 1. IEEE Press, 1992.

[5] K.C.-H Chao, S. Nadeem, W.L. Lee, and C.G. Sodini. A higher order topology for interpolative modulators for oversampling A/D converters. *IEEE Trans. Commun.*, 37(3):309–318, March 1990.

[6] J.H. Conway and N.J.A. Sloane. *Sphere Packings, Lattices and Groups*. Springer-Verlag, second edition, 1993.

[7] D.M. Divan. The resonant dc link converter–a new concept in static power conversion. In *IEEE IAS Ann. Meeting*, pages 648–656, Denver, 1986.

[8] R.M. Gray. Oversampled sigma-delta modulation. *IEEE Trans. Commun.*, COM-35(5):481–488, July 1987.

[9] T.G. Habetler and D.M. Divan. Performance characterization of a new discrete pulse modulated current regulator. In *IEEE IAS Ann. Meeting*, pages 395–405, Pittsburgh, October 1988.

[10] S. Hein and A. Zakhor. On the stability of sigma-delta modulators. *IEEE Trans. Signal Processiong*, 41(7):2322–2348, July 1993.

[11] J.J. Paulos, G.T. Brauns, M.B. Steer, and S.H. Ardalan. Improved signal to noise ratio using tri-level delta sigma modulation. In *Proc. IEEE Int. Symp. Circuits Syst.*, pages 463–466, Philadelphia, May 1987.

[12] R. Schreier. An empirical study of high order single bit delta sigma modulators. *IEEE Trans. Circuits Syst.*, 40(8):461–466, August 1993.

[13] D.R. Seidl. *System Identification and Control Using Structured Neural Networks*. PhD dissertation, University of Wisconsin-Madison, 1995.

[14] O. Shoaei and W.M. Snelgrove. Optimal (bandpass) continuous time $\Sigma\Delta$ modulator. In *Proc. IEEE Int. Symp. Circuits Syst.*, pages 489–492, London, May 1994.